13th World Conference on Earthquake Engineering
Vancouver, B.C., Canada
August 1-6, 2004
Paper No. 2925

RETROFIT OF LARGE BRIDGE PIERS WITH RECTANGULAR-HOLLOW CROSS-SECTION

Georgios TSIONIS[1] and Artur V. PINTO[2]

SUMMARY

The paper deals with the seismic retrofit of bridge piers with rectangular hollow cross-section using fibre-reinforced polymer (FRP) jackets. Finite element method (FEM) analyses show that the existing empirical laws for FRP-confined concrete are not suitable for hollow piers with large dimensions. The effectively confined zone is concentrated in the corners and its extent depends on the dimensions of the jacket. A fibre model of a hollow cross-section is analysed, modifying the concrete properties according to the aforementioned observations. The effectiveness of jacketing is conditioned by the axial load, longitudinal reinforcement and jacket dimensions. An empirical design equation is formulated.

INTRODUCTION

It has become clear from field observations and experimental data that existing bridge piers designed before the introduction of modern seismic codes are vulnerable to earthquakes and therefore appropriate retrofit solutions should be studied. This need is further accentuated by the significant economic loss related to serious damage or collapse of a major bridge and by the importance of bridge structures within complex transportation and communication systems. Particular attention is devoted in this work to bridge piers with hollow cross-section. Although this structural type is common in highway bridges across Europe and other seismic-prone regions, it has been the object of research only recently.

A sound background exists for the calculation of flexural and shear strength of reinforced concrete (RC) elements retrofitted with externally applied fibre-reinforced polymer (FRP) strips. Design equations and detailing rules have been proposed in research reports, e.g. Seible [1], and later incorporated in informative, *fib* [2], and normative documents, CEN [3]. No reference is made in these documents to piers with rectangular hollow cross-section. Recent experimental results from piers with hollow cross-sections retrofitted with FRP strips, reported by Ogata [4], Cheng [5] and Peloso [6], on one hand provide confidence in the effectiveness of the proposed design equations and techniques and on the other highlight the need for rational design rules, as some times FRP reinforcement is over-designed. However, the small scale of the tested specimens does not allow a generalisation of the observations.

[1]PhD student, Technical University of Milan, Department of Structural Engineering, Milan, Italy (formerly at JRC)
[2]Scientific officer, European Commission, Joint Research Centre, IPSC, ELSA, Ispra, Italy

Based on compression tests on concrete specimens encased in FRP jackets, a number of bilinear constitutive laws, with increasing stress for the second branch, have been proposed for FRP-confined concrete. In contrast, experimental evidence from specimens wrapped with a few FRP layers and/or specimens with rectangular cross-section indicate that the stress-strain curve comprises a softening post-peak branch with enhanced ultimate strain, as well as maximum and residual strength. The bilinear empirical models cannot capture this behaviour and the need for an alternative approach emerges. According to a theoretical model proposed by Spoelstra [7], the lateral strain of concrete is related to the axial strain and then an iterative procedure is followed until attainment of a given ultimate strain of the FRP. Design formulae have been proposed for the maximum strength and the ultimate strain of FRP-confined concrete. Based on these, Monti [8] elaborated design equations for the design of FRP jackets applied on circular RC columns.

A large number of constitutive laws for FRP-confined concrete have been examined by De Lorenzis [9]. The values estimated by the proposed empirical formulae were compared to the experimental values of strength and ultimate strain. The predictions for the ultimate strain were found to overestimate the experimental data, while errors ranging from 10% to 60% were observed on the values of compressive strength, often on the unconservative side. The discrepancies of the constitutive laws for FRP-confined concrete are reflected on the global response of elements, as highlighted in a numerical study of a circular RC cross-section wrapped with ten layers of FRP, performed by Yuan [10]. The results of moment-curvature analyses indicate significant differences in the predicted values of strength and ultimate curvature. While moment capacity is influenced mainly by concrete strength, curvature capacity directly depends on the ultimate strain of concrete. Concrete ultimate strain and cross-section curvature capacity are of great importance in seismic retrofit and hence it is unfortunate that a reliable model is not available yet.

The objective of the research presented in this paper is to examine the effectiveness of FRP jackets for the confinement of bridge piers with large hollow cross-sections. A two-level numerical approach is described. Analyses of a jacketed rectangular hollow concrete cross-section were performed using the Finite Element Method (FEM) with the aim of studying the effect of confinement on the concrete properties. The results of these analyses were incorporated in a fibre model of a RC cross-section and then parametric moment-curvature analyses were performed in order to study the effect of geometric and mechanical characteristics of the cross-section. The proposed numerical approach was checked against experimental evidence. Finally, empirical design equations were derived on the basis of more than 1000 numerical analyses.

EFFECT OF FRP JACKETS ON CONCRETE PROPERTIES OF HOLLOW CROSS-SECTIONS

The effect of the FRP jacket on the properties of concrete was examined by FEM analyses using the computer code Cast3m, Millard [11]. This was necessary because of the inconsistencies of existing constitutive laws for FRP-confined concrete and because of the limited confidence in their applicability to rectangular hollow cross-sections with large dimensions.

The width of the pier cross-section was b = 1.0 m and the depth d = 1.5b. The thickness of both the web and the flange was t = 0.2b. Five values were considered for the height of the concrete jacket, namely $h_j = 0.0$ (no concrete jacket), $h_j = 0.05$ m, $h_j = 0.10$ m, $h_j = 0.15$ m and $h_j = 0.20$ m. The thickness of the FRP jacket was $t_j = 1$ mm, $t_j = 3$ mm and $t_j = 5$ mm. In this way, a total number of 15 different cases were studied. The corner of the concrete cross-section was rounded at a radius of about 5 cm, as recommended for practical applications. For reasons of symmetry, only a fourth of the cross-section was analysed. Cubic elements with 8 or 6 integration points were used for the concrete cross-section, while

shell elements with 4 integration points were employed for the FRP jacket. The basic cross-section dimensions are given in Figure 1.

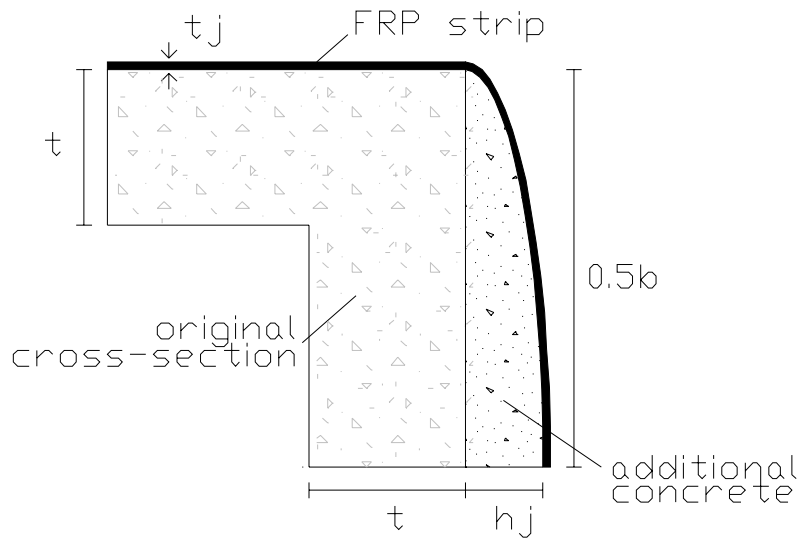

Figure 1. Definition of basic cross-section dimensions

A plasticity-based tri-dimensional constitutive law was used for the concrete elements (E_c = 33.5 GPa, ν = 0.2, f_c = 36 MPa and ε_o = 0.0025 for monotonic behaviour). Elastic behaviour was considered for the FPR jacket (E_{f1} = 52 GPa, E_{f2} = 5 GPa, ν = 0.2). It was decided to study a GFRP jacket, which is considered more effective for the enhancement of deformation capacity, rather than a CFRP jacket, which is more suitable for strength enhancement. Orthotropic behaviour was used to account for the presence of fibres only in the horizontal direction. The properties in the other direction were estimated considering the contribution of the matrix resin only. Elastic behaviour for the FRP elements is a limitation, as failure due to tensile fracture of the FRP strips (and explosive collapse of concrete) was not considered. Typical values of ultimate FRP strain can be higher than 3%, when measured through tensile tests. Experimental results from RC elements strengthened with FRP strips, though, indicate failure for smaller strains. To account for that, a safety factor in the order of 0.6 has been proposed by Seible [1] and *fib* [2]. This design value was not surpassed in the analyses. Perfect bond was considered between the two materials.

The effect of confinement within the cross-section is discussed with reference to Figure 2 in which the areas with the same compressive strength have the same colour. Dark blue colour corresponds to the smallest increase and changes to light blue, green, yellow and red for the areas with the highest increase. Zones with different extent of confinement may be identified. Zone 1 comprises the corner of the cross-section, without the external rounded part. A moderate increase in compressive and residual strength is observed in this zone. The external part of the corner, where the biggest increase is observed, is termed Zone 2. Zone 3 coincides with the flange, where a small increase in compressive and residual strength is observed. Finally, Zone 4 encompasses the additional concrete for the parabolic jacket. In this zone a small increase in strength is observed. The web is not considered to benefit from the retrofit.

For a rectangular jacket (top left in Figure 2) the effect of confinement is concentrated in the corner. For a parabolic jacket, also the area outside the corner benefits from the retrofit: the confined area extends from the corner to part of the web and the additional concrete. This effect is more pronounced for larger values of the jacket height, h_j. The effect of the jacket thickness is to increase the concrete strength, without

affecting the stress pattern. Similar observations hold also for the other properties of interest, which are discussed in the following.

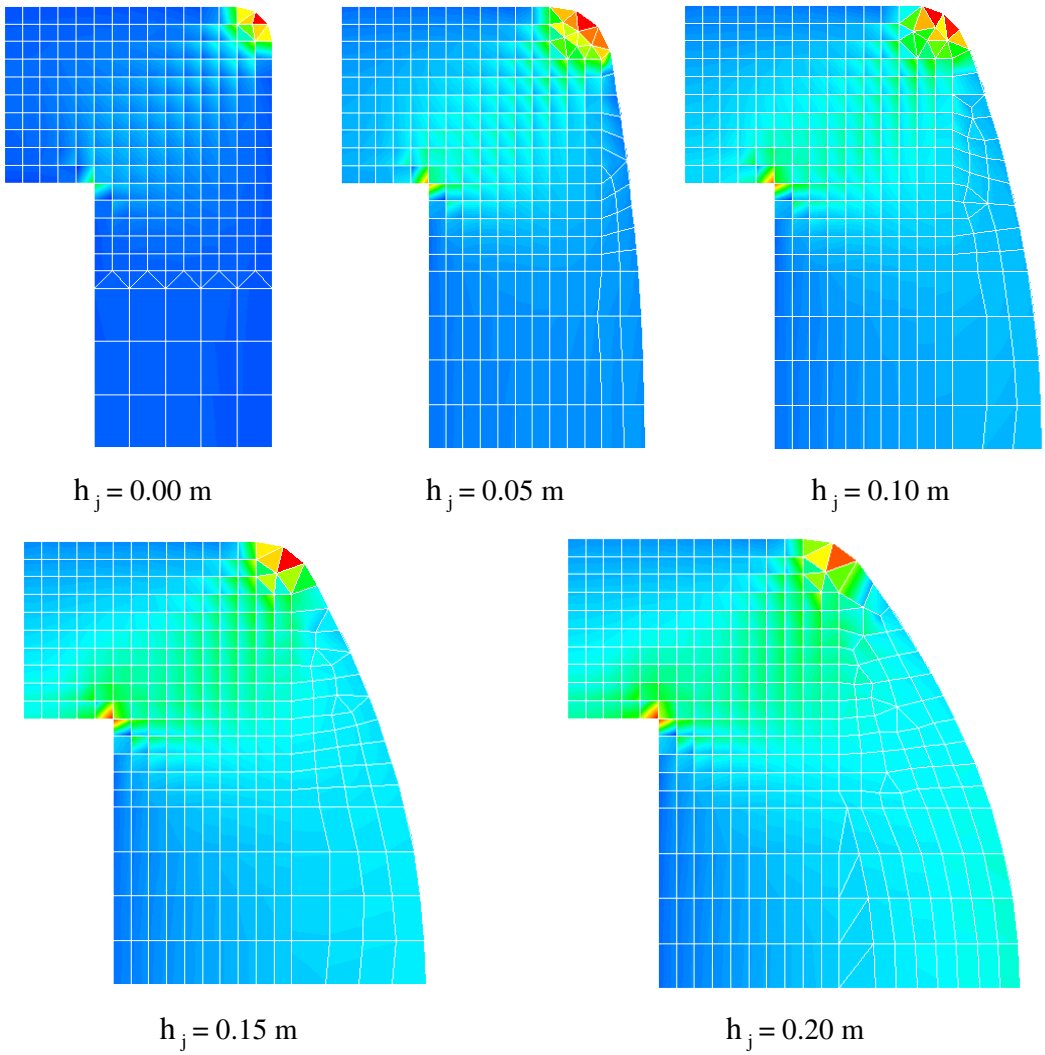

Figure 2. Effect of jacket height on the compressive strength of concrete (t_j = 5 mm)

Figure 3 plots indicative stress-strain curves in the different zones of the cross-section for a rectangular jacket and all three values of the jacket thickness. The curve for unconfined concrete is also included for comparison. The stress is obtained as the sum of the nodal reactions at each zone, divided by the area of the zone. Stresses are normalised to the compressive strength of unconfined concrete. The actual behaviour (softening after peak strength) does not follow the empirical relations proposed for FRP-confined concrete (bilinear law with ascending second branch). In fact, the effect of confinement is to increase the compressive and residual strength of concrete and to smooth the softening stiffness. This is reminiscent of the behaviour of full cross-sections confined with steel stirrups or jackets. Similar behaviour was experimentally observed on rectangular concrete specimens wrapped with few FRP strips, as reported by Karabinis [12]: the specimens showed softening after maximum strength, while increasing strength in the second branch was observed for higher amounts of FRP. In the numerical analyses, a bilinear stress-strain curve with increasing strength for the second branch was observed for extremely

high values of the jacket thickness that do not have practical application and also in a few elements close to the rounded corner. Nevertheless, this was not reflected on the global stress-strain curves for each zone.

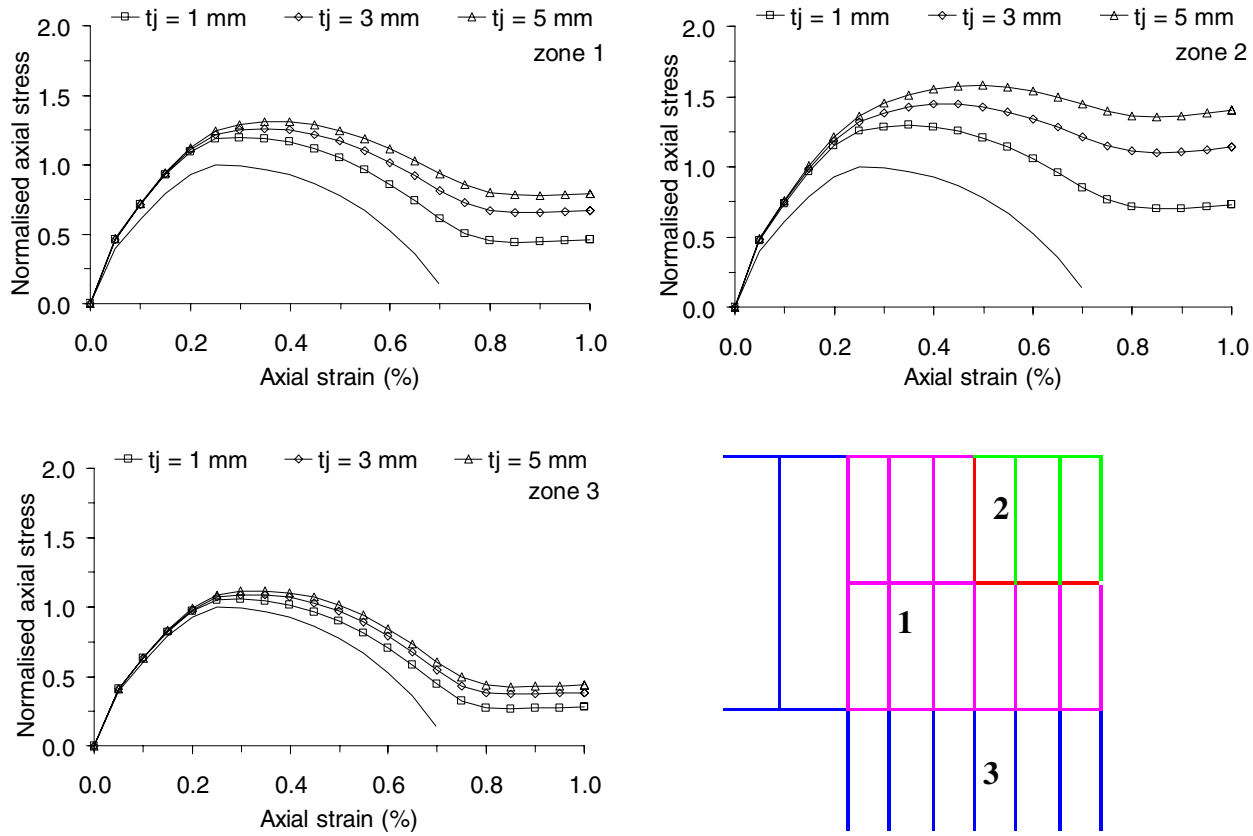

Figure 3. Numerical stress-strain curves for FRP-confined concrete (rectangular jacket) for uniform compressive forces and definition of zones (at the cross-section corner)

The numerical results are further discussed with focus on characteristic values of the stress-strain curves. The values of interest are the compressive strength, the residual strength and the softening stiffness. The softening stiffness is obtained as the difference of the maximum and residual strength, divided by the difference of the corresponding strains. These parameters, on one hand, give a qualitative view of the improvement of the concrete properties due to confinement. On the other hand, they are the material parameters used for the moment-curvature analyses described in the following section.

The effect of the jacket on the concrete compressive strength is discussed in more detail with reference to Figure 4, where stresses are normalised to the compressive strength of unconfined concrete. For all cases the concrete compressive strength increases with the jacket thickness, t_j. In Zones 1 and 3 the compressive strength is increased by 40% and 20%, respectively. In Zone 2 the compressive strength is increased by more than 80% for $t_j = 5$ mm. The compressive strength enhancement increases until $h_j =$ 0.10 m and then remains almost constant. Considering Zone 4, it is interesting to note that the compressive strength decreases with increasing values of the jacket height. The above observations suggest that a parabolic jacket of limited height is beneficial for the concrete properties, but when the jacket becomes relatively large, no further effect is obtained, or even a detrimental effect is observed. The value $h_j = 0.10$ m can be considered as an upper limit for the examined case.

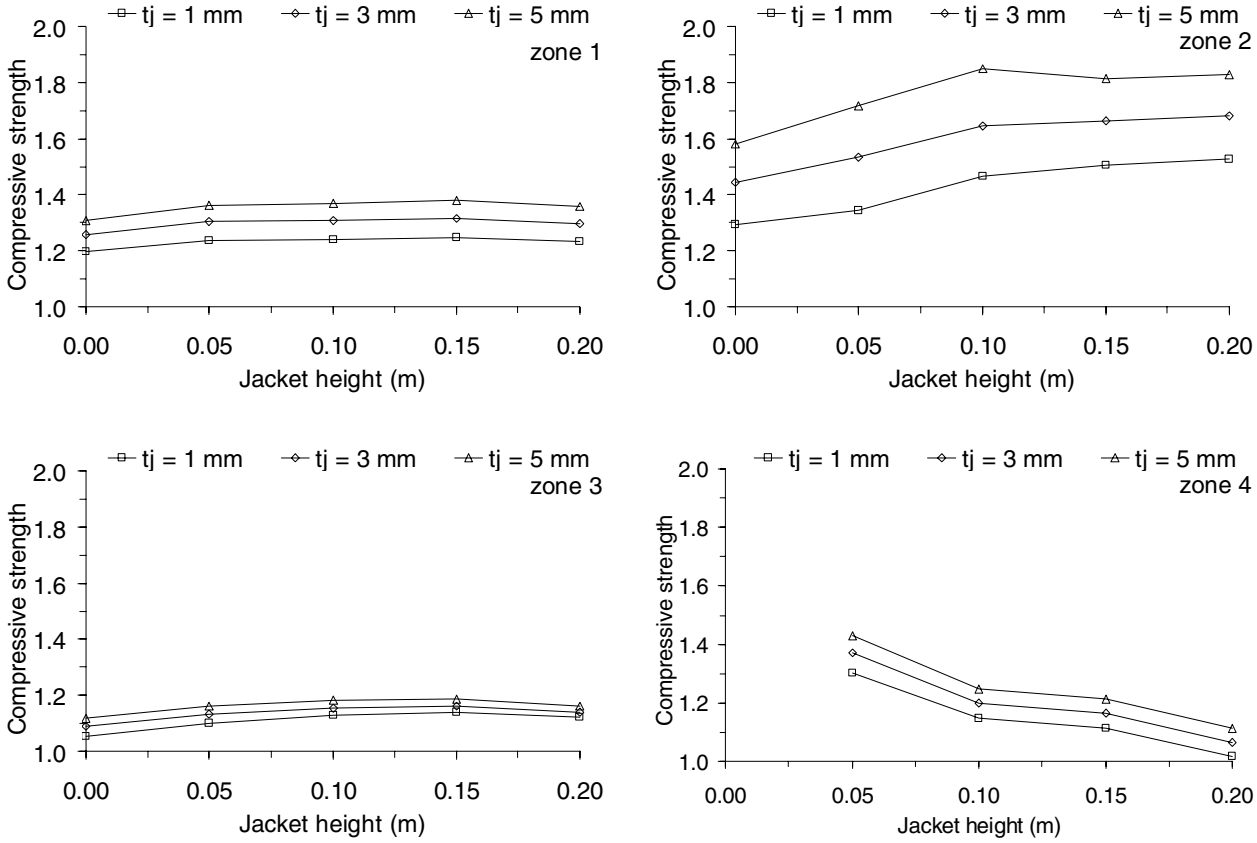

Figure 4. Effect of jacket on the compressive strength of concrete

Figure 5 plots the change of the concrete residual strength for different values of the jacket height and thickness. The residual strength is normalised to the compressive strength of unconfined concrete. The residual strength increases with the jacket thickness. The area that benefits more is again the region near the rounded corner. Moderate improvement is observed in Zones 1 and 4, while in Zone 3 the residual strength remains at less that $0.6 f_c$. An interesting feature is that for small amount of FRP, $t_j = 1$ mm, the improvement does not increase with the jacket height. Also for the residual strength, no further improvement is obtained for jackets with height larger than $h_j = 0.10$ m. The softening stiffness decreases with the jacket height. The decrease is faster until $h_j = 0.10$ m and then no change, or slower decrease is observed.

EFFECT OF FRP JACKETS ON CURVATURE DUCTILITY OF HOLLOW CROSS-SECTIONS

Moment-curvature analyses were performed using the finite element code Cast3m, Millard [11], with the aim to study the effect of the jacket dimensions, axial load and reinforcement ratio on the effectiveness of the retrofit. Non-linear behaviour was considered for the concrete fibres and a modified Menegotto-Pinto constitutive law for the steel fibres, both described by Guedes [13]. The FRP jacket was not included in the model. In lieu, the cross-section was divided in five zones (the fifth zone is the web, which is not considered to experience any confinement effect) with properties modified in accordance to the results of the FEM analyses. An equivalent I cross-section was analysed, instead of the original rectangular hollow cross-section. Rectangular elements with four integration points and triangular elements with three integration points where used for the concrete fibres and point elements with one integration point were

employed for the steel rebars. The steel fibres were positioned at the external and internal faces of the flanges, as well as through the web: 20% of vertical reinforcement was concentrated at the external face of the flanges, 10% was concentrated at the internal face of the flanges and the remaining 70% was distributed along the web.

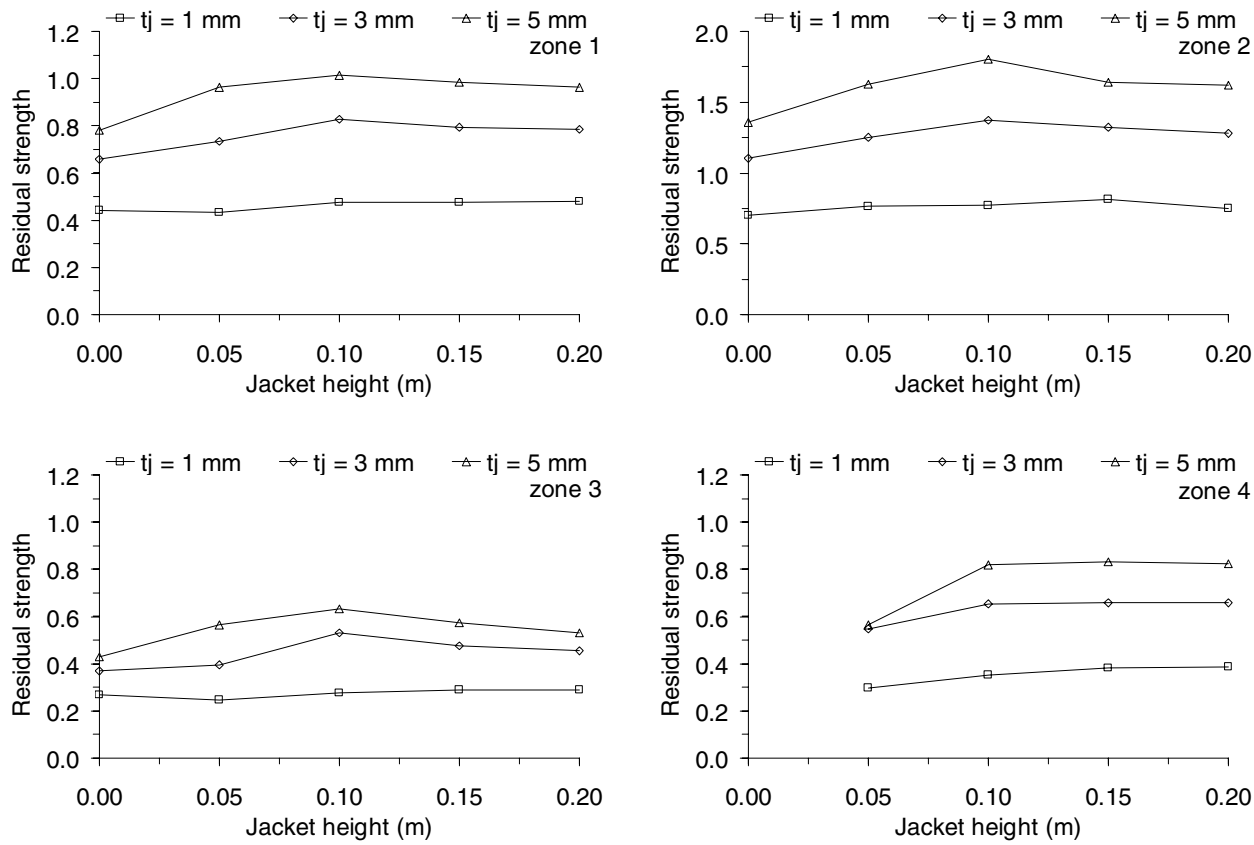

Figure 5. Effect of jacket on the residual strength of concrete

Different values of axial load (ranging from $\nu = 0.0$ to $\nu = 0.3$) and longitudinal reinforcement ratio ($\rho_s =$ 0.17%, $\rho_s = 0.34\%$, $\rho_s = 0.68\%$ and $\rho_s = 1.02\%$) were considered. Curvature ductility is defined by way of a bilinear approximation of the actual moment-curvature diagram. The yield moment is equal to the maximum moment, M_{max}. The yield curvature is defined at the intersection of a line from the origin passing through the numerical curve at $0.8\,M_{max}$ and a horizontal line at M_{max}. The ultimate curvature is conservatively defined at M_{max}, see Figure 7a.

Selected results are plotted in Figure 6 for a jacket of height $h_j = 0.10$ m. For both the as-built and retrofitted cross-sections, increase of axial load initially increases the curvature ductility. This range of axial load corresponds to failure of the cross-section due to collapse of steel, as indicated by rapid loss of resistance in the moment-curvature diagrams. After a certain value, further increase of axial load, causes decrease of curvature ductility. This range of axial load corresponds to failure of the cross-section due to crushing of concrete, as indicated by smooth decrease of resistance after the peak in the moment-curvature diagrams. The limit value of axial load ranges from $\nu_N = 0.0$ to $\nu_N = 0.1$ for the as-built cross-

section and from $\nu_N = 0.05$ to $\nu_N = 0.2$ for the jacketed cross-section, depending on the dimensions of the jacket and the longitudinal reinforcement ratio. As expected, curvature ductility decreases with increasing reinforcement ratio.

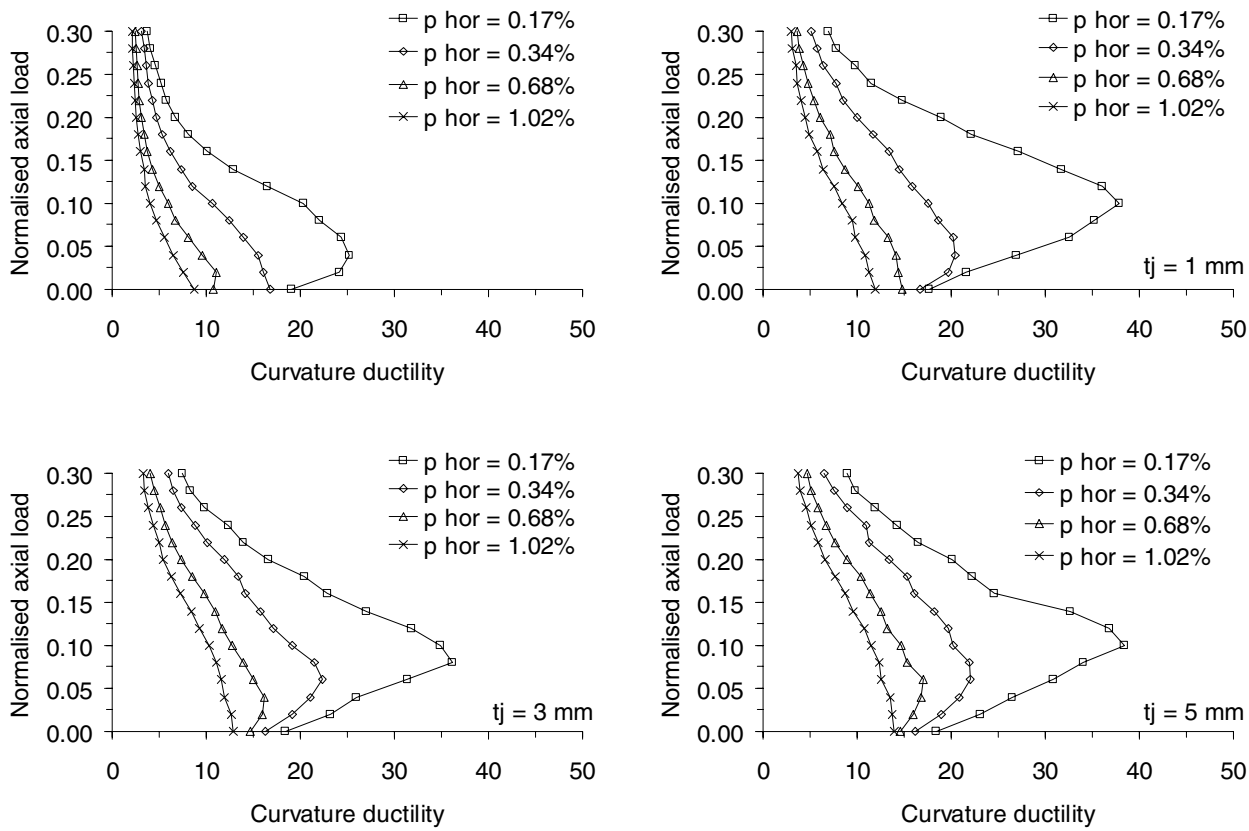

Figure 6. Effect of jacket, axial load and longitudinal reinforcement ratio on the curvature ductility of the cross-section (h_j = 0.10 m)

The ratio of the curvature ductility of the jacketed cross-section to the curvature ductility of the as-built cross-section can be used as an effectiveness index. The effect of axial load is to initially increase the effectiveness of the retrofit and then to decrease it. The limit value of the axial load depends on the amount of longitudinal reinforcement, jacket thickness and jacket height. For low to medium amounts of vertical reinforcement (from $\rho_s = 0.17\%$ to $\rho_s = 0.68\%$) jacketing is not effective for piers with very low values of axial load, namely $\nu_N < 0.05$. In these cases, large tension strains develop in the steel before significant compression on the concrete and failure is due to collapse of steel. For higher amounts of longitudinal reinforcement jacketing is effective even for low values of axial load. The numerical results clearly indicate that this retrofit method is most effective for medium to high axial loads, namely in the range from $\nu_N = 0.1$ to $\nu_N = 0.3$.

Among the examined cases, the maximum value of the effectiveness index was $\mu_{\varphi,\text{retrofitted}} / \mu_{\varphi,\text{as-built}} = 3.7$, for a jacket with height $h_j = 0.20$ m and thickness $t_j = 5$ mm. It is important at this point to recall that ultimate curvature is conservatively defined at maximum moment, as schematically shown in Figure 7a.

This definition is adopted because it renders it possible to derive design-oriented empirical expressions that have relatively good correlation with the numerical values. Although this might lead in over-dimensioning at certain cases, the results remain on the safe side. Values of the effectiveness index as high as $\mu_{\varphi,\text{retrofitted}} / \mu_{\varphi,\text{as-built}} = 7.0$ are obtained if ultimate curvature is defined at the point of the moment-curvature diagram where there is a 20% loss of strength, as shown in Figure 7b. This definition is more realistic and demonstrates the actual effectiveness of the retrofit method. The first definition is kept in the following for consistency.

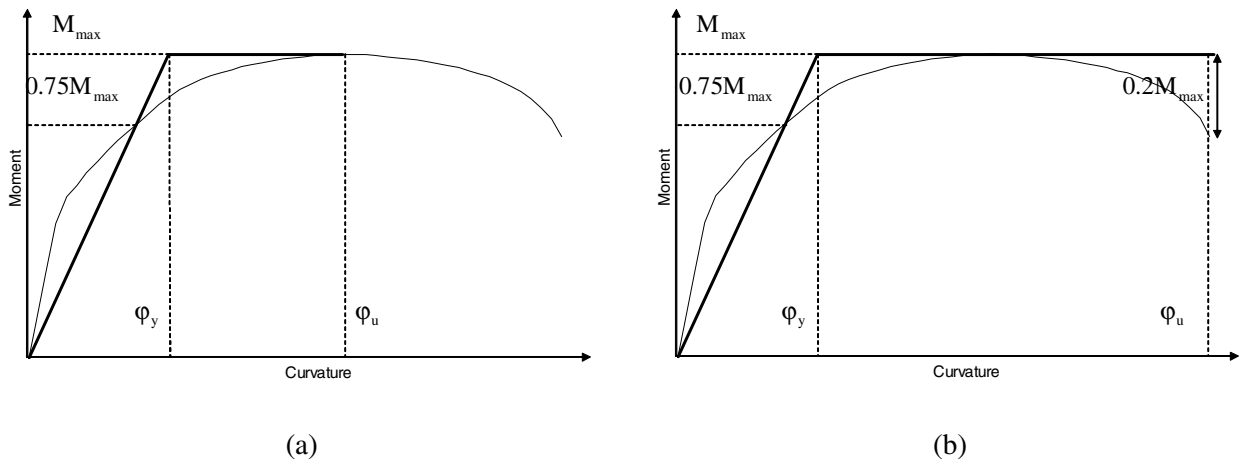

Figure 7. Definition of failure criteria and curvature ductility: at maximum moment (a) and at 20% loss of strength (b)

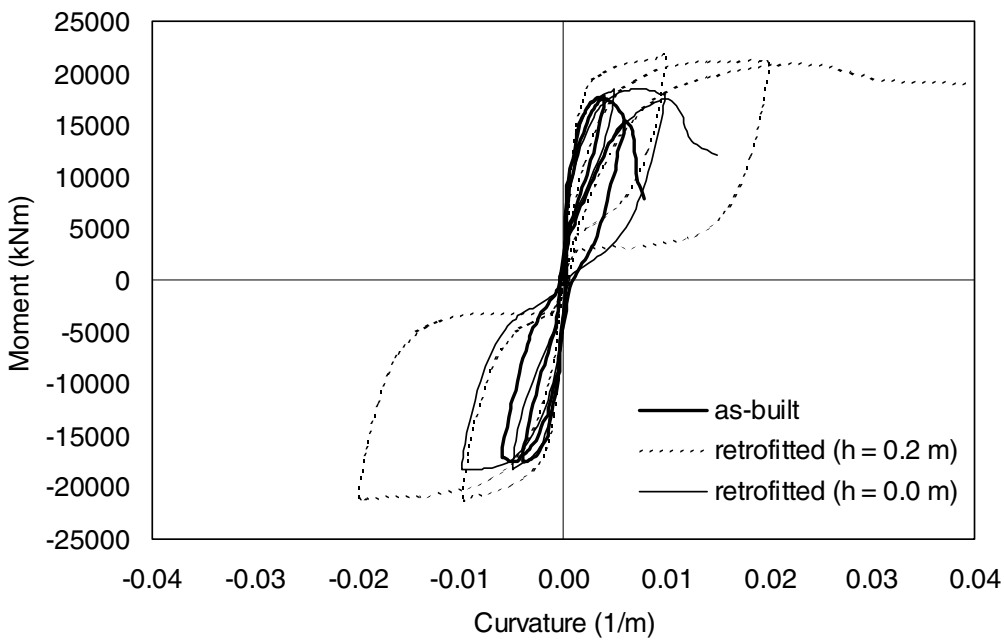

Figure 8. Cyclic moment-curvature diagrams for the as-built and jacketed cross-section

For the examined cases, the maximum increase of moment capacity is about 20%. When increasing the dimensions of the cross-section, an increase of stiffness is expected. A member with increased stiffness

will attract higher seismic forces and this fact has to be taken into consideration when designing the global retrofit. This increase will also affect the dynamic properties, which are significant for bridge structures. Jacketing will decrease the usually high periods of bridge piers and then most probably will increase the spectral ordinates and accordingly the seismic demand. The above correspond to increase in shear demand that might exhaust the as-built capacity and strengthening will be required. Retrofit of the foundation might be needed.

The effect of FRP jacketing on the energy dissipation capacity is verified in Figure 8 that plots the moment-curvature numerical curves for $\nu_N = 0.2$, $\rho_s = 1.02\%$, $t_j = 5$ mm and the two extreme values of the jacket height. For the case of rectangular jacket and the same level of imposed curvature, no significant difference is observed between the as-built and the retrofitted cross-sections. Nevertheless, the retrofitted cross-section has a much higher curvature ductility, which can be exploited also under cyclic loading. For higher values of the concrete jacket, both strength and ultimate curvature increase and then a more pronounced dissipation capacity is evidenced by the wider hysteretic cycles.

COMPARISON TO EXPERIMENTAL RESULTS

The experimental results of a small-scale specimen of a pier retrofitted with longitudinal and transversal GFRP strips tested at the University of Pavia are compared in this section to the results of the numerical procedure described in the previous sections. The scaled specimen had a rectangular hollow cross-section with external dimensions 0.45x0.45 m and internal dimensions 0.35x0.35 m. The longitudinal reinforcement consisted of 40 $\Phi 8$ rebars uniformly distributed along the internal and external faces of the pier, corresponding to reinforcement ratio $\rho_s = 0.025$. The horizontal reinforcement consisted of one rectangular stirrup for each wall of the specimen, vertically spaced at 0.075 m. The compressive strength of concrete was $f_c = 30.3$ MPa. The yield stress of steel was $f_y = 550$ MPa, while the ultimate stress was $f_u = 660$ MPa. The as-built specimen failed due to combination of flexure and shear at drift $\delta = 3.6$ %.

The retrofit intervention consisted in applying longitudinal and transversal GFRP strips. Two longitudinal layers of 0.1 m-wide strips were applied on both faces orthogonal to the loading direction. The transversal strips had the same width and the spacing was 0.2 m from centre to centre. Compared to the as-built specimen, the retrofitted specimen showed larger deformation capacity ($\delta = 6.0$ %), stable response and larger capacity of energy dissipation. A detailed description of the geometry, materials and experimental behaviour is given by Peloso [6].

Following the numerical procedure described previously, the concrete cross-section wrapped with the FRP strips was analysed under increasing compressive load. The thickness of the FRP strips was modified in order to take into consideration the effect of partial wrapping. While continuous jackets exert a constant lateral pressure along the height of the element, partial wrapping is less efficient as parts of the concrete remain unconfined. A confinement effectiveness coefficient is used, based on the assumption that the unconfined zone between two consecutive strips is enclosed by a parabola with 45° slope [2].

The effect of wrapping is to increase the maximum strength and the corresponding deformation. The numerical results indicate that for the examined case a softening branch, with smoother slope compared to unconfined concrete, follows the point of maximum compressive stress, until a residual strength. While plain concrete is considered to have nil residual strength, the values for FRP-confined concrete range from $0.3 f_c$ to $0.8 f_c$ in the different zones of the cross-section. Confinement results also in increase of the concrete pseudo-ductility, as seen by the deformation capacity of FRP-confined concrete, compared to unconfined concrete.

The effect of confinement is restricted to the corner of the cross-section. Apart from a stress concentration at the external part of the corner, consistent with experimental observations, the cross-section may be divided in three regions. One comprises the part outside the corner, where the maximum strength is not increased, but the residual strength is $f_{r1} = 0.2f_c$. The second area corresponds to the external part of the corner, where the maximum strength is increased by 10% and the residual strength is $f_{r2} = 0.75f_c$. In this zone an ascending branch initiates at strain levels of about 0.7%. This is reminiscent of the second branch of the empirical bilinear constitutive laws for FRP-confined concrete. In the following analyses this branch will be ignored and constant residual stress, f_{r2}, will be considered. Finally, the third zone comprises the remaining part of the corner, where the maximum strength remains unchanged and the residual strength is $f_{r3} = 0.5f_c$. These values hold for the given geometry; more general considerations were discussed in the previous section.

The numerical stress-strain curves were used to define the properties of the concrete fibres in a fibre/Timoshenko beam element, Guedes [13], used to model the retrofitted pier. The horizontal FRP strips were not included in the model, but their effect was accounted for by appropriately modifying the concrete properties in the three regions of the cross-section. The longitudinal FRP strips were modelled using four-point quadrangular elements with equivalent area, positioned on the two faces of the cross-section. An elastic-perfectly plastic constitutive law was considered for the longitudinal strips in order to impose a limit on the strength of the longitudinal strips, corresponding to the nominal maximum stress. Numerical simulation considering elastic behaviour of the longitudinal strips showed that the strength constantly increased with displacement, even after many concrete fibres had collapsed.

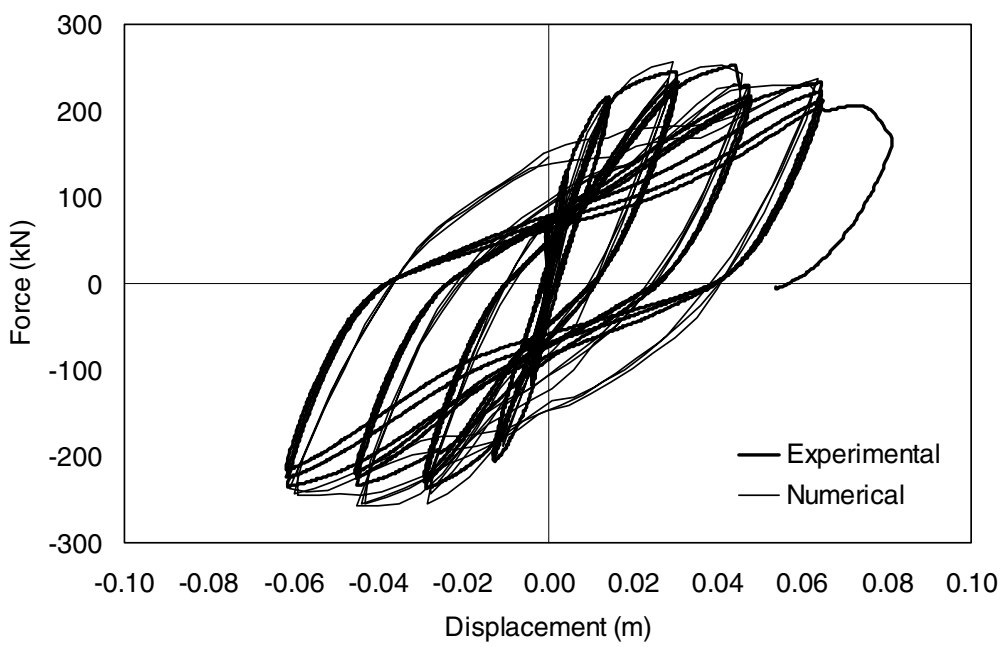

Figure 9. Experimental and numerical force-displacement curves

The complete model was used to simulate the cyclic test on the retrofitted specimen. The numerical and experimental force-displacement curves are compared in Figure 9, where good agreement is observed. The resistance and degradation predicted by the numerical model are close to the experimental values. Some differences are observed in the reloading branches of the cycles of large amplitude. The pinching

response of the tested pier can be attributed to the opening and closing of cracks in the concrete and also to inelastic shear deformation, both of which are not fully considered in the numerical analysis. These differences result in higher energy dissipation in the numerical model. Note that the differences are localised on the cycles with large displacement, $\delta > 4.8\%$, where relatively important shear deformation and big crack openings are expected.

The comparison between the numerical and experimental results serves as a validation for the numerical tools and their combination. The numerical simulations yield rational results, which are able to interpret the experimental behaviour of the tested specimen. The experimental results verify the effectiveness of FRP jackets for upgrading of bridge piers with hollow cross-section. The agreement between the numerical and experimental global results provides confidence in the numerical tools and procedure.

DESIGN EQUATIONS

Graphs similar to those presented in Figure 6 may be used to dimension the jacket for a given cross-section and a target value of curvature ductility. The objective of this section is to derive empirical design equations for FRP jackets applied on bridge piers with rectangular hollow cross-sections. The design equations are based on the numerical results presented previously. The design of the jacket is seen as a step within a global retrofit procedure. The term global refers to the consideration of all possible failure modes. Considering RC bridge piers, the main seismic deficiencies, which have been reported from field observations and laboratory testing, are premature termination of vertical reinforcement, lapped splices within the potential plastic hinge region, inadequate confinement (small deformation and dissipation capacities) and inadequate shear capacity. Quite often, existing bridge piers present a combination of the aforementioned seismic deficiencies. Nevertheless, only the weakest of them is the main cause of failure. It is obvious that if the objective of the retrofit intervention is to provide resistance against the weakest mechanism only, then most probably failure will be due to the second weakest mode. This is the reason to introduce the global retrofit procedure. Jacketing is proposed as a method to increase confinement.

An expression of curvature ductility as a function of the examined geometrical and mechanical characteristics of the cross-section (axial load, longitudinal reinforcement ratio, height and thickness of the jacket) is sought. These characteristics are grouped in a single design parameter, termed $S = f(\nu_N, h_j, t_j, \rho_s)$ in the following, and then an expression in the form $\mu_\varphi = f(S)$ is fitted to the numerical results. The empirical equations take the form

$$\mu_{\varphi,m} = 52.94 \exp\left[\frac{-6.86(0.1+\nu_N)^{0.7}(1+h_j)^{0.1}\rho_s^{0.3}}{(1+t_j)^{0.2}}\right] \tag{1}$$

$$\mu_{\varphi,0.05} = 42.35 \exp\left[\frac{-8.10(0.1+\nu_N)^{0.7}(1+h_j)^{0.1}\rho_s^{0.3}}{(1+t_j)^{0.2}}\right] \tag{2}$$

$$S = \frac{(0.1+\nu_N)^{0.7}(1+h_j)^{0.1}\rho_s^{0.3}}{(1+t_j)^{0.2}} \tag{3}$$

In the previous equations ν_N is the normalised axial load, h_j is the jacket height (in m), t_j is the jacket thickness (in mm) and ρ_s is the longitudinal reinforcement ratio (in %). The normalised axial load,

$\nu_N = P / A_c f_c$, and the ratio of longitudinal reinforcement, $\rho_s = A_s / A_c$, are defined for the original rectangular cross-section without the jacket, A_c. P is the axial force, f_c is the nominal compressive strength of concrete and A_s is the area of steel rebars. $\mu_{\varphi,m}$ is the mean value, while $\mu_{\varphi,0.05}$ is the 5% characteristic value (95% of the empirical values are lower than the corresponding numerical values). The numerical values are plotted in Figure 10, along with Equations 1 and 2. The correlation factor for Equation 1 is $R^2 = 0.81$.

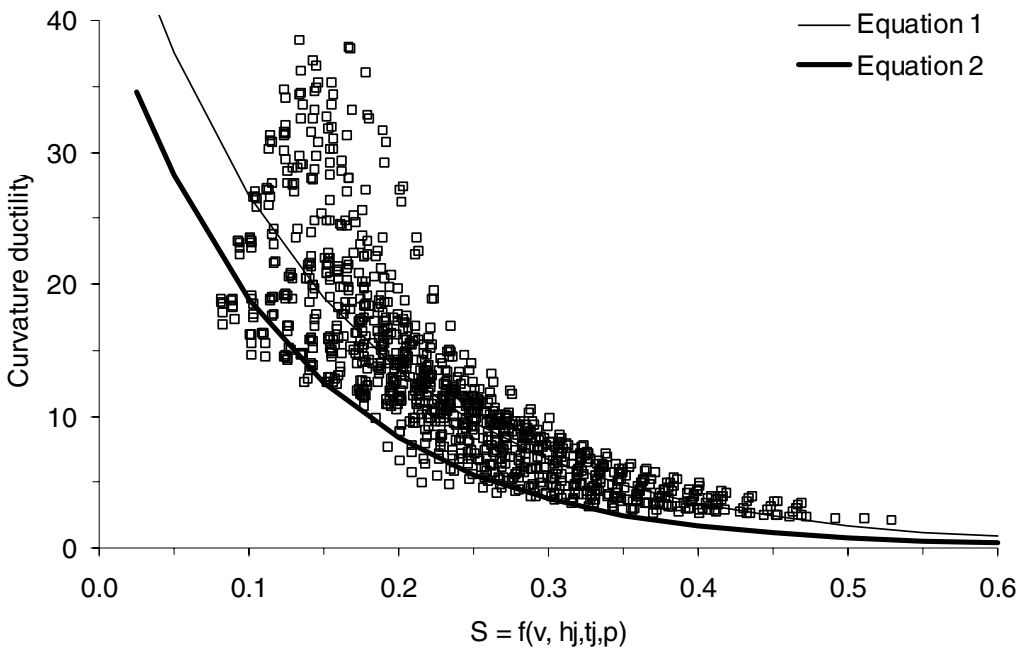

Figure 10. Empirical fit to the numerical values of curvature ductility

The effectiveness index is defined as the ratio of curvature ductility of the retrofitted cross-section to that of the as-built one. Starting from this definition and using Equation 2, one obtains

$$I_{0.05} = \frac{\mu_{\varphi,\text{retrofitted},0.05}}{\mu_{\varphi,\text{as-built},0.05}} = 0.6\exp\left\{8.1(0.1+\nu_N)^{0.7}\rho_s^{0.3}\left[1-\frac{(1+h_j)^{0.1}}{(1+t_j)^{0.2}}\right]\right\} \quad (4)$$

Due to the relatively poor correlation, a modification is included in Equation 4 to obtain the 5% characteristic value of the effectiveness index (95% of the empirical values are lower than the numerical values). The empirical and numerical values are compared in Figure 11.

In Equations 1 to 4 there are two unknown design parameters, namely jacket height and thickness. This means that one has to select one of them and then enter the design formulae with this value and the desired value of curvature ductility, or effectiveness index, in order to calculate the other. It might be preferable to limit the jacket height so as not to increase the strength and stiffness of the retrofitted member. The limit $h_j = 0.10$ m, identified in this study, may be considered. Besides, it might be desired to limit the jacket thickness in order to avoid practical problems related to the superposition of many FRP layers. The above imply an iterative procedure and require some engineering judgement.

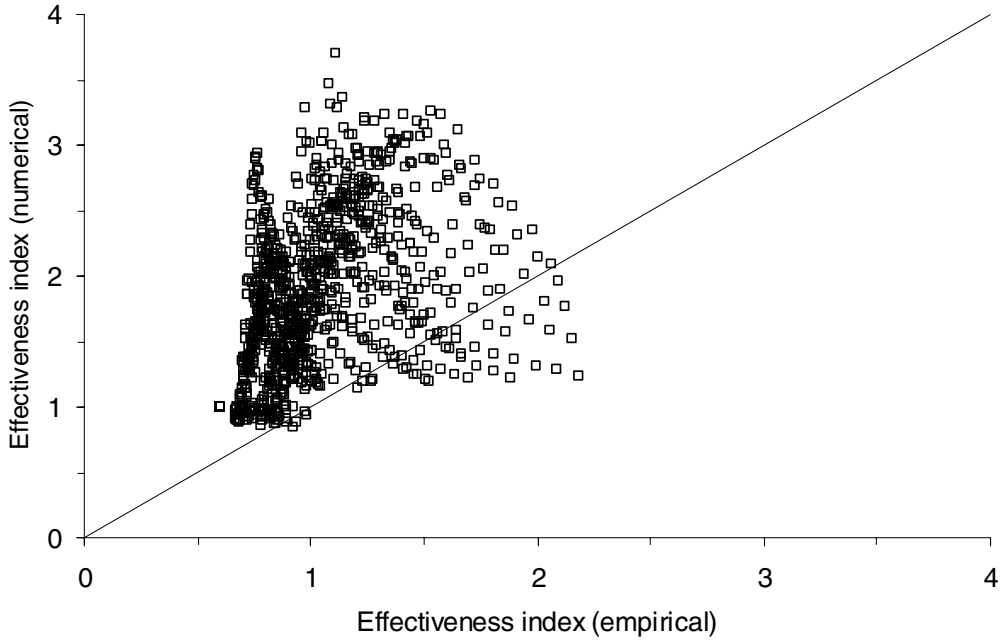

Figure 11. Empirical (5% characteristic) and numerical values of the effectiveness index

The empirical design equations derived in this section can be used when the geometrical and mechanical characteristics of the piers fall within the limits examined in the present study. Considering axial load, longitudinal reinforcement ratio, jacket height and thickness, it is believed that the whole range of practical interest has been examined. For piers with dimensions smaller than those examined in this study, the jacket dimensions may be scaled down and conservative results will be obtained. The design formulae should not be used for piers with larger dimensions because it is expected that confinement will not be the same effective and then the proposed equations might provide unsafe results.

CONCLUSIONS

FEM analyses of a concrete cross-section wrapped with an FRP jacket suggest that for the case of hollow piers with large dimensions and for realistic dimensions of the jacket, the stress-strain curve after the peak strength comprises a softening branch with a slope less steep than the one for unconfined concrete. Maximum and residual strength are increased with respect to unconfined concrete. Distinct zones of the cross-section with different effect of confinement have been identified. For rectangular jackets, the effectively confined zone is limited to the corners, where peak and residual strength are notably improved. For elliptical jackets, moderate improvement is observed also in part of the flange and added concrete. A limit value of the jacket height, after which the concrete properties are not further improvement, was identified.

The effectiveness of jacket for the enhancement of the deformation capacity of RC cross-sections is conditioned by the axial load, longitudinal reinforcement and dimensions of the jacket. The jackets are most effective in the range of axial load from $\nu_N = 0.1$ to $\nu_N = 0.3$, which, luckily, corresponds to the axial loads bridge piers usually carry. The moment capacity of the cross-section is increased by about 20%. This results in higher forces and then shear strengthening and upgrade of the foundation might be required. FRP jackets improve the cyclic behaviour of cross-sections and therefore higher energy dissipation capacity is ensured.

On the grounds of extended numerical studies and limited experimental results, it is concluded that, keeping in mind the aforementioned limitations, parabolic FRP jackets constitute an effective method for improving the seismic response of poorly-detailed hollow bridge piers.

AKNOWLEDGEMENTS

The greatest part of this work was carried out under a JRC grant (Contract No. 15775-2000-03 P1B20 ISP IT) to the first author and within the SAFERR Research Training Network (Contract No. HPRN-CT-1999-00035). The support of the European Commission is acknowledged.

REFERENCES

1. Seible F, Priestley MJN, Innamorato D. "Earthquake retrofit of bridge columns with continuous carbon fiber jackets – Volume II, Design guidelines." Report No. ACTT-95/08, San Diego: Structural Engineering, University of California, San Diego, 1995.
2. *fib*. "Design and use of externally bonded FRP reinforcement for reinforced concrete structures." Lausanne: Fédération Internationale du Béton, 2001.
3. CEN. "Eurocode 8: Design of structures for earthquake resistance – Part 3: Strengthening and repair of buildings (Draft No 3)." Brussels: Comité Européen de Normalisation, 2003.
4. Ogata T, Osada K. "Seismic retrofitting of expressway bridges in Japan." Cement and Concrete Composites 2000; 22(1): 17-27.
5. Cheng CT, Yang JC, Yeh YK, Chen SE. "Seismic performance of repaired hollow-bridge piers." Construction and Building Materials 2003; 17(5): 339-351.
6. Peloso S. "FRP seismic retrofit of square hollow section bridge piers." MSc dissertation, Pavia: ROSE School, Università degli Studi di Pavia, 2003.
7. Spoelstra MR, Monti G. "FRP-confined concrete model." ASCE Journal of Composites for Construction 1999; 3(3): 143-150.
8. Monti G, Nisticò N, Santini S. "Design of FRP jackets for upgrade of circular bridge piers." ASCE Journal of Composites for Construction 2001; 5(2): 94-101.
9. De Lorenzis L. "A comparative study of models on confinement of concrete cylinders with FRP composites." Work No 46, Publication 01:04, Göteborg: Chalmers University of Technology, 2001.
10. Yuan XF, Lam L, Teng JG, Smith ST. "FRP-confined RC columns under combined bending and compression: a comparative study of concrete stress-strain models". Teng JG, Editor. FRP Composites in Civil Engineering. Amsterdam: Elsevier Science Ltd, 2001: 749-758.
11. Millard A. "Castem 2000, Guide d' utilisation." Rapport CEA 93/007. Saclay: CEA, 1993.
12. Karabinis AI, Rousakis TC. "Behaviour of rectangular FRP confined concrete elements subjected to monotonic and cyclic compressive load". Proceedings of the *fib* 2003 Symposium: Concrete Structures in Seismic Regions, Athens, Greece. Paper no. 112. Athens: Technical Chamber of Greece, 2003.
13. Guedes J, Pegon P, Pinto AV. "A fibre/Timoshenko beam element in CASTEM 2000." JRC Special publication I.94.31, Ispra: European Commission, Joint Research Centre, 1994.